Security Classification

DOCUMENT CONTROL DATA - R & D

(Security classification of title, body of abstract and indexing annotation must be entered when the overall report is classified)

1. ORIGINATING ACTIVITY (Corporate author)	2a. REPORT SECURITY CLASSIFICATION
Naval Research Laboratory	Unclassified
	2b. GROUP

3. REPORT TITLE

ON THE STATISTICS OF SEA CLUTTER

4. DESCRIPTIVE NOTES *(Type of report and inclusive dates)*

A final report on one phase of a continuing NRL problem.

5. AUTHOR(S) *(First name, middle initial, last name)*

G.R. Valenzuela and M.B. Laing

6. REPORT DATE	7a. TOTAL NO. OF PAGES	7b. NO. OF REFS
December 30, 1971	38	23

8a. CONTRACT OR GRANT NO.	9a. ORIGINATOR'S REPORT NUMBER(S)
NRL Problem R02-37	
b. PROJECT NO.	NRL Report 7349
A310310B/652A/A R02101-002	
c. (formerly A310310B/652A/1 R008-01-020)	9b. OTHER REPORT NO(S) *(Any other numbers that may be assigned this report)*
d.	

10. DISTRIBUTION STATEMENT

Approved for public release; distribution unlimited.

11. SUPPLEMENTARY NOTES	12. SPONSORING MILITARY ACTIVITY
	Department of the Navy (Naval Air Systems Command), Washington, D.C. 20360

13. ABSTRACT

A model for the statistics of sea clutter has been developed from scattering theory and the composite surface-scattering model. The model postulates that sea clutter is exponentially (Rayleigh envelope) distributed for glassy seas and should tend toward the lognormal distribution (in particular for horizontal polarization) with increasing roughness. The lognormality of sea clutter arises from the tilting of the slightly rough "patches" by the large-scale roughness (undulating surface).

An empirical identification of the statistics of sea clutter taken with the Four-Frequency Radar system shows that in general the distribution of sea clutter is intermediate between the exponential (Rayleigh envelope) and the lognormal distribution. However, for calm seas and small sample sizes (less than about 200 independent samples) the distribution of sea clutter may be approximated by either the exponential or the lognormal distribution.

The first five central moments of sea clutter (in decibels) have been calculated for moderate and rough sea conditions.

DD FORM 1 NOV 65 1473 (PAGE 1)

S/N 0101-807-6801

Security Classification

14. KEY WORDS	LINK A		LINK B		LINK C	
	ROLE	WT	ROLE	WT	ROLE	WT
Sea clutter						
Statistical model						
Scattering theory						
Composite surface						
Probability distribution functions						
Probability density functions						
Lognormal clutter						
Kolmogorov-Smirnov test						
Independent Samples						
Moments						

TABLE OF CONTENTS

	Page
Abstract	ii
Problem Status	ii
Authorization	ii
INTRODUCTION	1
THEORETICAL CONSIDERATIONS	2
The Radar Detection Problem	2
Electromagnetic Scattering from Rough Surfaces	3
STATISTICAL MODEL OF SEA CLUTTER	6
IDENTIFICATION OF THE STATISTICS OF SEA CLUTTER OBTAINED WITH THE NRL-4FR SYSTEM	15
The Distribution Function	15
The Central Moments	17
DISCUSSION OF RESULTS AND CONCLUSIONS	26
ACKNOWLEDGMENTS	33
REFERENCES	33

ABSTRACT

A model for the statistics of sea clutter has been developed from scattering theory and the composite surface-scattering model. The model postulates that sea clutter is exponentially (Rayleigh envelope) distributed for glassy seas and should tend toward the lognormal distribution (in particular for horizontal polarization) with increasing roughness. The lognormality of sea clutter arises from the tilting of the slightly rough "patches" by the large-scale roughness (undulating surface).

An empirical identification of the statistics of sea clutter taken with the Four-Frequency Radar system shows that in general the distribution of sea clutter is intermediate between the exponential (Rayleigh envelope) and the lognormal distribution. However, for calm seas and small sample sizes (less than about 200 independent samples) the distribution of sea clutter may be approximated by either the exponential or the lognormal distribution.

The first five central moments of sea clutter (in decibels) have been calculated for moderate and rough sea conditions.

PROBLEM STATUS

This is a final report on one phase of the problem; work on other phases is continuing.

AUTHORIZATION

NRL Problem R02-37
Project A310310B/652A/A R02101-002
(formerly A310310B/652A/1 R008-01-020)

Manuscript submitted September 10, 1971.

ON THE STATISTICS OF SEA CLUTTER

INTRODUCTION

Radar detection, which is a binary detection problem (i.e., the selection of one outcome from two events), has developed quite rapidly since the early 1940's and its progress can be followed in Middleton (1). However, modern radar detection theory is not considered to have started until the Marcum (2) and Swerling (3) contributions, and presently it has reached a high level of maturity. Nevertheless, most formal developments still only treat explicitly the detection of signals (deterministic or random) strictly in Gaussian noise (4).

Unfortunately, many of the geophysical noises encountered in practice are non-Gaussian (e.g., atmospheric disturbances, terrain, and sea clutter), and to implement realistic detection schemes the true statistics of these geophysical noises must be identified a priori.

Recently it has been suggested that the statistics of sea clutter, in particular for high-resolution radars and toward grazing incidence, cannot be expressed as a Rayleigh distribution (exponential in power) but can be approximated by other distributions, among them the lognormal distribution (5).

The main purpose of this investigation is to identify the statistical properties of sea clutter, both by electromagnetic scattering theory via the composite surface-scattering model (6, 7) and empirically by statistical analysis of sea clutter taken with the Four-Frequency Radar (4FR) system (8), which transmits at 428 MHz (P band or UHF), 1228 MHz (L band), 4455 MHz (C band), and 8910 MHz (X band). The composite surface-scattering model already has been quite successful in predicting the mean value of sea clutter (9-11) and explaining the width of the doppler spectrum of radar sea echo (12). The potential of this scattering model to derive other statistical information of sea clutter is to be explored here.

Anticipating some of the results to be obtained later, it is possible to say that the tilting of the slightly rough "patches" by the large-scale roughness (i.e., the undulating surface) is the mechanism that generates the non-Rayleigh statistics observed in sea clutter, in particular for horizontal polarization. Also in the empirical identification of sea clutter taken with the 4FR system by the Kolmogorov-Smirnov test on the cumulative distribution and by the computation of the first five central moments, the distribution of sea clutter (for a radar pulsewidth of 0.5 μsecond) is found to be intermediate between the exponential (Rayleigh envelope) and the lognormal distribution, and these distributions may serve as the limiting distributions of sea clutter.

THEORETICAL CONSIDERATIONS

The Radar Detection Problem

In binary detection problems the Bayes criterion is used (1, 4) when the a priori probabilities and cost functions of making a decision are known (i.e., the risk in making the wrong decisions is minimized). The implementation of the Bayes criterion in detection leads to a likelihood ratio test

$$\Lambda(V) = \frac{p(V/H_1)}{p(V/H_0)} > \lambda, \text{ if } H_1 \text{ is true,} \tag{1a}$$

and

$$\Lambda(V) = \frac{p(V/H_1)}{p(V/H_0)} < \lambda, \text{ if } H_0 \text{ is true,} \tag{1b}$$

where $p(V/H_1)$ and $p(V/H_0)$ are the conditional probability densities given that event H_1 is true (signal plus noise are present) and given that event H_0 is true (noise alone is present), respectively. The threshold level λ is a function of the cost functions and the a priori probabilities of the sources.

Since, in practice, the cost functions and the a priori probabilities are not known, other criteria must be considered. In radar detection, the Neyman-Pearson criterion is most frequently used, the probability of false alarm P_F is specified, and the probability of detection P_D is maximized.

The threshold level under these constraints is obtained from

$$P_F = \int_{\lambda}^{\infty} p(V/H_0)\, dV, \tag{2}$$

and the required signal-to-noise ratio required for detection then is obtained from

$$P_D = \int_{\lambda}^{\infty} p(V/H_1)\, dV. \tag{3}$$

The implementation of the Neyman-Pearson criterion also leads to a likelihood ratio test similar to Eq. (1) with the threshold level now being determined from Eq. (2).

Thus, for radar systems operating in the sea environment the conditional probability density of clutter must be known in order to have realistic estimates of the probability of false alarm as a function of radar and sea parameters. Other criteria for detection also exist (1, 4), but they will not be discussed here.

Integration of several radar pulses should improve the performance of detection, the amount of improvement depending on the correlation properties of clutter alone in relation to the correlation properties of signal plus clutter.

Electromagnetic Scattering from Rough Surfaces

Consider the scattering properties of a statistical rough surface, with surface currents $\mathbf{K}_e = \mathbf{n} \times \mathbf{H}$ and $\mathbf{K}_m = -\mathbf{n} \times \mathbf{E}$ due to a plane wave incident on the surface (Fig. 1). The scattered fields may be obtained by means of the following integral equation formulation (13, 14), where the time dependence is taken to be $e^{i\omega t}$ and the unit normal vector $\mathbf{n}$ is pointing toward free space:

$$\mathbf{E}_s(\mathbf{r}) = \int_s ds' \, \mathbf{K}_m(\mathbf{r}') \times \nabla' G(\mathbf{r},\mathbf{r}') - \frac{i\omega\mu_0}{k^2} \nabla \times \int_s ds' \, \mathbf{K}_e(\mathbf{r}') \times \nabla' G(\mathbf{r},\mathbf{r}') \tag{4}$$

$$\mathbf{H}_s(\mathbf{r}) = -\int_s ds' \, \mathbf{K}_e(\mathbf{r}') \times \nabla' G(\mathbf{r},\mathbf{r}') + \frac{1}{i\omega\mu_0} \nabla \times \int_s ds' \, \mathbf{K}_m(\mathbf{r}') \times \nabla' G(\mathbf{r},\mathbf{r}'), \tag{5}$$

where ω is the electromagnetic frequency in radians, μ_0 is the magnetic permeability, k is the propagation constant of a plane wave in free space, $G(\mathbf{r},\mathbf{r}')$ is the Green's function in free space, and $\mathbf{r}'$ is the radius vector for a point on the rough surface.

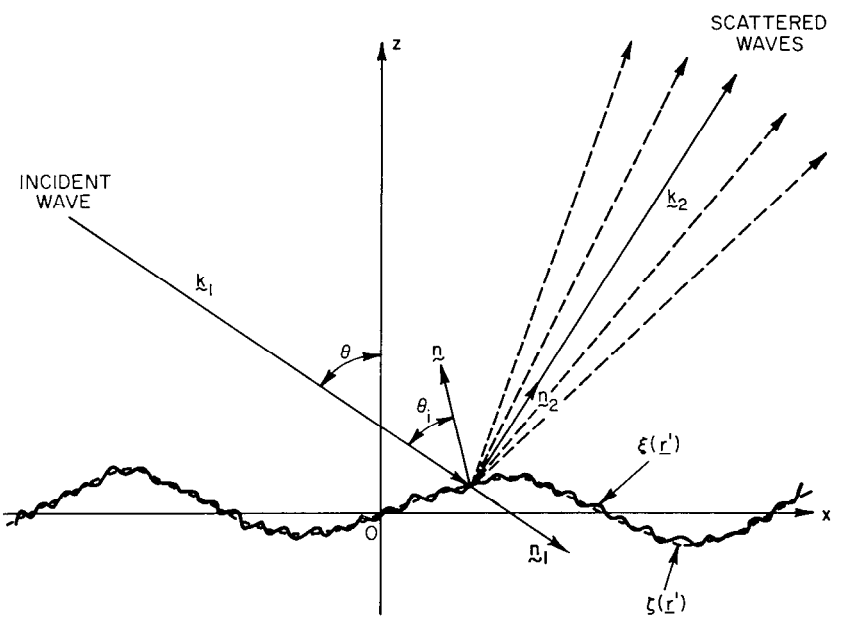

Fig. 1—Scattering geometry

The integral equations (4) and (5) can be simplified for the "far field" (i.e., all scattered rays arriving in a given direction must be propagating parallel to each other). In this case, the following approximations apply

$$\nabla' G(\mathbf{r},\mathbf{r}') = \nabla' \left(\frac{e^{-ik|\mathbf{r}-\mathbf{r}'|}}{4\pi|\mathbf{r}-\mathbf{r}'|} \right) \approx ikG(\mathbf{r},\mathbf{r}')\mathbf{n}_2 \tag{6}$$

$$G(R,\mathbf{r}') = \frac{e^{-ikR}}{4\pi R} e^{ik\,2\cdot\mathbf{r}'} \tag{7}$$

$$\nabla \times \mathbf{K}_e(\mathbf{r}') \times \nabla' G(\mathbf{r},\mathbf{r}') = -\nabla \times \nabla' G(\mathbf{r},\mathbf{r}') \times \mathbf{K}_e(\mathbf{r}') \approx -k^2 \mathbf{n}_2 \times (\mathbf{n}_2 \times \mathbf{K}_e) G(\mathbf{r},\mathbf{r}'), \tag{8}$$

where $\mathbf{k}_2$ is the propagation vector of the scattered wave, R is the distance from the observation point to the origin of the coordinates system, and $\mathbf{n}_2 = \mathbf{k}_2/k$.

Using the approximations given in Eqs. (4) and (5), the following equations result:

$$\mathbf{E}_s(R) \approx \mathcal{K} \left\{ \int ds' \, \mathbf{n}_2 \times [\mathbf{K}_m(\mathbf{r}') + Z_0 \mathbf{n}_2 \times \mathbf{K}_e(\mathbf{r}')] e^{ik\,2\cdot\mathbf{r}'} \right\} \tag{9}$$

$$\mathbf{H}_s(R) \approx -\mathcal{K} \left\{ \int ds' \, \mathbf{n}_2 \times [\mathbf{K}_e(\mathbf{r}') - Y_0 \mathbf{n}_2 \times \mathbf{K}_m(\mathbf{r}')] e^{ik\,2\cdot\mathbf{r}'} \right\}, \tag{10}$$

where

$$\mathcal{K} = \frac{ike^{-ikR}}{4\pi R}, \; Z_0 = \sqrt{\mu_0/\epsilon_0} = 120\Omega, \text{ and } Y_0 = 1/Z_0.$$

Accordingly, the statistics of the scattered fields depend only on the statistics of the surface currents and the statistic properties of the rough surface.

Letting

$$\mathbf{L} = \int ds' \, \mathbf{K}_m(\mathbf{r}') e^{ik\,2\cdot\mathbf{r}'} \tag{11}$$

$$\mathbf{M} = \int ds' \, \mathbf{K}_e(\mathbf{r}') e^{ik\,2\cdot\mathbf{r}'}, \tag{12}$$

the magnitude square of the fields (which is proportional to power) is given by

$$|\mathbf{E}_s \cdot \mathbf{p}|^2 \approx \left(\frac{k}{4\pi R} \right)^2 \left\{ |\mathbf{L}\cdot(\mathbf{p}\times\mathbf{n}_2)|^2 + Z_0^2 |\mathbf{M}\cdot\mathbf{p}|^2 + 2Z_0 \Re e(\mathbf{M}\cdot\mathbf{p})[\mathbf{L}^*\cdot(\mathbf{p}\times\mathbf{n}_2)] \right\} \tag{13}$$

and

$$|\mathbf{E}_s \cdot (\mathbf{n}_2 \times \mathbf{p})|^2 \approx \left(\frac{k}{4\pi R} \right)^2 \left\{ |\mathbf{L}\cdot\mathbf{p}|^2 + Z_0^2 |\mathbf{M}\cdot(\mathbf{n}_2\times\mathbf{p})|^2 + 2Z_0 \Re e(\mathbf{L}^*\cdot\mathbf{p})[\mathbf{M}\cdot(\mathbf{n}_2\times\mathbf{p})] \right\}, \tag{14}$$

where $\mathbf{L}^*$ is the complex conjugate vector of $\mathbf{L}$ and $\mathbf{p}$ is a polarization unit vector such that $\mathbf{p}\cdot\mathbf{n}_2 = 0$.

For a rough surface of impedance Z_s, the magnetic surface current $\mathbf{K}_m(\mathbf{r}')$ can be obtained from the electric surface current $\mathbf{K}_e(\mathbf{r}')$ by

$$\mathbf{K}_m(\mathbf{r}') = -Z_s \mathbf{n}(\mathbf{r}') \times \mathbf{K}_e(\mathbf{r}'). \tag{15}$$

The surface currents $\mathbf{K}_e$ and $\mathbf{K}_m$ are determined from the boundary value problem of the air/rough surface interface from the incident electromagnetic wave on the surface. When the scattering surface is statistically rough, the boundary value problem cannot be solved in closed form, and accordingly appropriate approximations must be used for the surface currents.

Fortunately, for rough surfaces like the sea, which has a two-dimensional spectrum $W(\mathbf{K})$ of the form K^{-4} (K is the wavenumber of the surface roughness or waves), a slightly rough local boundary condition may be used. This fundamentally separates the sea surface into large-scale roughnesses (undulating surface) and small-scale roughnesses (Bragg resonant scatterers). According to the local-slightly rough boundary condition, the surface fields on the undulating surface (i.e., $\zeta(\mathbf{r}')$) may be expressed as a function of the small-scale roughness (i.e., $\xi(\mathbf{r}')$),

$$\mathbf{H}(\mathbf{r}') = \mathbf{h}[\mathbf{n}(\mathbf{r}'), \mathbf{k}_1, Z_s]\, \xi(\mathbf{r}') e^{-i\mathbf{k}_1 \cdot \mathbf{r}'}, \tag{16}$$

where now $\mathbf{n}(\mathbf{r}')$ becomes the unit normal vector to $\zeta(\mathbf{r}')$, the undulating surface. The Soviets have used a similar approach (15).

Substituting Eqs. (15) and (16) in Eq. (9) and specializing for backscatter, $\mathbf{k}_2 = -\mathbf{k}_1$ and $\mathbf{n}_2 = -\mathbf{n}_1$, the following approximation is derived:

$$\mathbf{E}_s^B \approx \mathbb{K}\, \mathbf{n}_1 \times \int [\mathbf{n}_1 + Z_s \mathbf{n}(\mathbf{r}')] \times [\mathbf{n}(\mathbf{r}') \times \mathbf{h}(\mathbf{r}')]\, \xi(\mathbf{r}') e^{-2i\mathbf{k}_1 \cdot \mathbf{r}'} ds'. \tag{17}$$

The integration in Eq. (17) can be performed in the following sequence: first, integrate over each slightly rough surface "patch" and then add the contributions from the "patches"

$$\mathbf{E}_s^B \approx \mathbb{K} \sum_{\text{patches}(p)} \left\{ \mathbf{n}_1 \times [\mathbf{n}_1 + Z_s \mathbf{n}(p)] \times [\mathbf{n}(p) \times \mathbf{h}(p)]\, e^{-2k_{1z}(p)} \zeta(p) \right.$$
$$\left. \int_{(p)} \xi(\mathbf{r}') e^{-2i(k_{1x} x' + k_{1y} y')}\, d(\text{patch}) \right\}. \tag{18}$$

The backscattered power P_s^B, which is proportional to $|E_s^B|^2$, is given by

$$P_s^B \propto \sum_{p,\ell} \left\{ \mathbf{n}_1 \times [\mathbf{n}_1 + Z_s \mathbf{n}(p)] \times [\mathbf{n}(p) \times \mathbf{h}(p)] \right\} \left\{ \mathbf{n}_1 \times [\mathbf{n}_1 + Z_s \mathbf{n}(\ell)] \times [\mathbf{n}(\ell) \times \mathbf{h}(\ell)] \right\}^* \cdot$$

$$e^{-2i[k_{1z}(p)\zeta(p) - k_{1z}(\ell)\zeta(\ell)]} \int_{(p)} \int_{(\ell)} \xi(\mathbf{r}')\xi^*(\mathbf{r}'')$$

$$e^{-2i[k_{1x'}(p)x' - k_{1x''}(\ell)x'' + k_{1y'}(p)y' - k_{1y''}(\ell)y'']}\, d(p)d(\ell), \tag{19}$$

where x',y' are in patch(p) and x'',y'' are in patch (ℓ).

Neglecting the cross terms (the contribution from two different patches), basically assumes that the fields from different patches are independent and the backscatter power will be given by

$$P_s^B \propto \sum_{(p)} \left\{ |\mathbf{n}_1 \times [\mathbf{n}_1 + Z_s \mathbf{n}(p)] \times [\mathbf{n}(p) \times \mathbf{h}(p)]|^2 \cdot \right.$$

$$\left. \iint_{(p)} \xi(\mathbf{r}')\xi^*(\mathbf{r}' + \Delta\mathbf{r}') e^{-2[k_{1x'}\Delta x' + k_{1y'}\Delta y']}\, d(\Delta x')d(\Delta y') \right\} \cdot \tag{20}$$

Thus, for an incident plane wave when the slightly rough-local boundary condition is used, the backscattered power from a rough surface is given by Eq. (19). If the contributions from the various "patches" are mutually independent, the backscattered power may be approximated by Eq. (20), which can be given the same physical interpretation as the composite surface-scattering model formulation as proposed by Wright (6). This last result will be the basis for the statistical model of sea clutter to be developed in the following section.

Here it is appropriate to indicate that this analysis applies for an incident plane wave. In practical applications the incident electromagnetic radiation originates from an aperture of finite dimensions, and the incident electromagnetic radiation is a superposition of many plane waves. Accordingly, the backscattered power should include an additional summation over the spectrum of the incident plane waves.

STATISTICAL MODEL OF SEA CLUTTER

As shown previously, the scattering results for certain types of rough surfaces, in particular for the sea, can be simplified considerably by the assumptions of the composite surface-scattering model. It is recalled that the assumption of incoherent addition has been used (power adds) in contrast with coherent addition in which the fields from the various slightly rough "patches" add.

The backscattered power from each "patch" is the product of two factors: one factor is purely a function of the electrical properties of the surface and the local geometry, and another factor is a function of the energy of the small-scale roughness $\xi(\mathbf{r}')$; refer to Eq. (20). Thus, if the illuminated area is of approximately one "patch" (i.e., narrow pulse and narrow antenna beam case), sea-clutter statistics may be modeled by a product of two random variables:

$$Z = XY, \tag{21}$$

where X is a random variable dependent on the slopes of the large-scale roughness, ζ' and Y is another random variable dependent on the statistics of the small-scale roughness ξ. The variables X and Y here are taken to be mutually independent.

Accordingly, the probability density functions (pdfs) of the random variables X and Y should be of the forms

$$p(X) = p(\zeta') \left| \frac{d\zeta'}{dX} \right| \tag{22}$$

and

$$p(Y) = e^{-Y}, \tag{23}$$

where the mean value of Z has been included in X.

The reason for selecting these two pdfs should become more obvious as we proceed. Equation (22) follows directly from the law of transformation of pdfs, and Eq. (23) is the pdf of the energy spectral density of the small-scale roughness, which is assumed to be Gaussian in amplitude. Therefore, the pdf of the random variable Z, according to elementary probability theory, should be given by (16)

$$p(Z) = \int_0^\infty \frac{1}{X} p(X) p\left(Y = \frac{Z}{X}\right) dX. \tag{24}$$

For the case involving illumination of several "patches" at one time (wide-pulse and wide-antenna beams), sea-clutter statistics may be represented by the sum random variable.

$$Z_t = Z_1 + Z_2 + \ldots + Z_n. \tag{25}$$

Clearly, the conditional density $p(V/H_0)$ used in calculating the probability of false alarm in Eq. (2) is Eq. (24) for the narrow-pulse and narrow-antenna beam or the pdf of the random variable in Eq. (25) for the wide case.

A detailed development follows for the simpler case of single "patch" illumination. The random variable X in Eq. (21) can readily be identified with the normalized radar cross section obtained for slightly rough scattering theory (7), thus (to first order), for horizontal polarization

$$X(\theta_i)_H = 4\pi k^4 \cot^4 \theta_i |\alpha^2 \cos^2 \delta T_{\perp\perp} + \sin^2 \delta [\epsilon(1+\alpha_i^2) - \alpha_i^2] T_{\parallel\parallel}|^2 \cdot$$

$$W(2k\alpha, 2k\gamma \sin \delta), \tag{26}$$

and (to first order) for vertical polarization

$$X(\theta_i)_V = 4\pi k^4 \cot^4 \theta_i |\alpha^2 \cos^2 \delta [\epsilon(1+\alpha_i^2) - \alpha_i^2] T_{\parallel\parallel} + \sin^2 \delta T_{\perp\perp}|^2 \cdot$$

$$W(2k\alpha, 2k\gamma \sin \delta), \tag{27}$$

where

$$\gamma_i = \cos \theta_i = \cos(\theta + \psi) \cos \delta, \alpha_i = (1-\gamma_i^2)^{1/2}, \alpha = \sin(\theta + \psi), \gamma = (1-\alpha^2)^{1/2},$$

$$T_{\perp\perp} = \frac{\epsilon - 1}{(\gamma_i + \gamma'')^2}, T_{\parallel\parallel} = \frac{\epsilon - 1}{(\epsilon\gamma_i + \gamma'')^2}, \gamma'' = (\epsilon - \alpha_i^2)^{1/2},$$

ϵ is the complex dielectric constant of the surface, $W(K_x, K_y)$ is the two-dimensional spectrum of the small-scale roughness of the "patch" (i.e.,

$$\overline{\xi^2} = (1/4) \int\int_{-\infty}^{\infty} W(K_x, K_y)\, dK_x\, dK_y),$$

which is taken to be constant on each "patch," and ψ and δ are the "tilt" angles with respect to the horizontal plane, parallel and perpendicular to the plane of incidence, respectively.

To have a unique relationship between X and slope ζ', side tilts cannot be included in this formulation. Thus, in this statistical model, only tilts parallel to the plane of incidence are to be included. Letting $\delta = 0$ in Eqs. (26) and (27), gives

$$X(\theta_i)_H = 4\pi k^4 \cos^4 \theta_i \left| \frac{(\epsilon - 1)}{(\cos \theta_i + \sqrt{\epsilon - \sin^2 \theta_i})^2} \right|^2 W(2k \sin \theta_i, 0) \tag{28}$$

and

$$X(\theta_i)_V = 4\pi k^4 \cos^4 \theta_i \left| \frac{(\epsilon - 1)[\epsilon(1 + \sin^2 \theta_i) - \sin^2 \theta_i]}{(\epsilon \cos \theta_i + \sqrt{\epsilon - \sin^2 \theta_i})^2} \right|^2 W(2k \sin \theta_i, 0). \tag{29}$$

The slopes of the undulating surface are Gaussian distributed,

$$p(\zeta') = \frac{1}{\sqrt{2\pi} S} e^{-(\zeta')^2/2S^2}, \tag{30}$$

and since $\tan \psi = -\zeta'$, the pdf of X can be found from Eq. (22) using Eq. (30) and Eqs. (28) or (29). Let $W(K_X, K_Y) = 6 \cdot 10^{-3} K^{-4}$ and initially take the case of a perfectly conducting sea, (where, $\epsilon = -i\infty$). Then, Eqs. (28) and (29) become

$$X(\theta_i)_H = C \cot^4 \theta_i \tag{31}$$

and

$$X(\theta_i)_V = C (\cot^2 \theta_i + 2)^2, \tag{32}$$

where $C = (3\pi/2) \cdot 10^{-3}$.

After some straightforward algebra, for a perfectly conducting sea the pdfs for the random variables X are

$$p(X_H) \propto \frac{\sec^2 \tau}{4CS\sqrt{2\pi}} \cdot \frac{e^{-\frac{1}{2S^2}\left(\frac{A-\tan\tau}{1+A\tan\tau}\right)^2}}{A^3(1 + A \tan \tau)^2} \tag{33}$$

and

$$p(X_V) \propto \frac{\sec^2 \tau}{4CS\sqrt{2\pi}} \cdot \frac{e^{-\frac{1}{2S^2}\left(\frac{B-\tan\tau}{1+B\tan\tau}\right)^2}}{B(B^2 + 2)(1 + B \tan \tau)^2}, \tag{34}$$

where $\tau = 90^\circ - \theta$ (grazing angle), $A = (X_H/C)^{1/4}$, and $B = [(X_V/C)^{1/2} - 2]^{1/2}$. The constants of proportionality in Eqs. (33) and (34) are obtained from the normalization of the pdf.

In Figures 2 through 5, Eq. (33) has been plotted for various grazing angles and rms slopes of the undulating surface. As observed the pdf of X_H is nearly Gaussian for small S and tends to the exponential distribution for large S. For small grazing angles the tail of the pdf increases with large S, a characteristic of the lognormal distribution; so seemingly we have found that the lognormal properties of sea clutter may be explained in terms of the tilting of the slightly rough patches by the large-scale roughness.

The probability distribution corresponding to Eq. (33) is

$$P(X > X_H) \propto \frac{1}{2}\left[Erf\left(\frac{\cot \tau}{\sqrt{2}S}\right) \mp Erf\left(\frac{|\tan \psi|}{\sqrt{2}S}\right)\right], \tag{35}$$

where the upper sign applies for $\tan \psi \geqslant 0$ and the lower sign applies for $\tan \psi < 0$, $\tan \psi = A - \tan \tau / 1 + A \tan \tau$ and

$$Erf\,(...) = \frac{2}{\sqrt{\pi}} \int_0^{(...)} e^{-t^2}\, dt.$$

Equation (35) has been plotted in Fig. 6 for $\tau = 40^\circ$ and for several values of S. Figure 7 gives same curves plotted on normal probability paper, where lognormal distributions plot

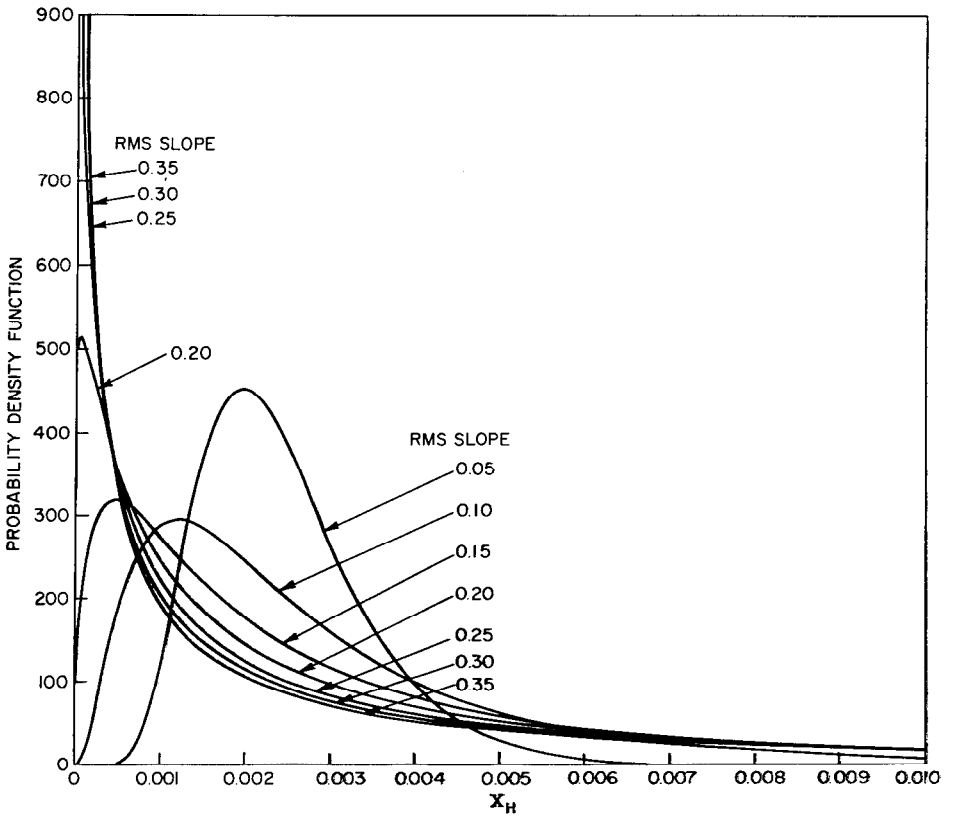

Fig. 2—Density function of X_H for perfectly conducting sea and 40-degree grazing angle

as straight lines. These curves indicate that the distribution of X_H has lognormal characteristics, which is most evident for small S, and for large S the tail of the distribution increases with increasing S.

The pdf and the distribution function for X_V for a perfectly conducting sea are not too interesting because Eq. (32) approaches a constant toward the grazing incidence. Thus, to obtain realistic results for the distributions of X_V the more exact expression Eq. (29), which applies for a sea surface of finite conductivity, must be used. The pdf and the probability distribution for X_H will not change drastically for the case of finite, but large conductivity.

From the functional dependence of Eqs. (28) and (29) on the angle of incidence and tilt angle, the inverse of those expressions can be approximated by the series

$$\tan(90^\circ - \theta_i) = \sum_{\ell=1}^{N} a_\ell X^{\ell/N}, \tag{36}$$

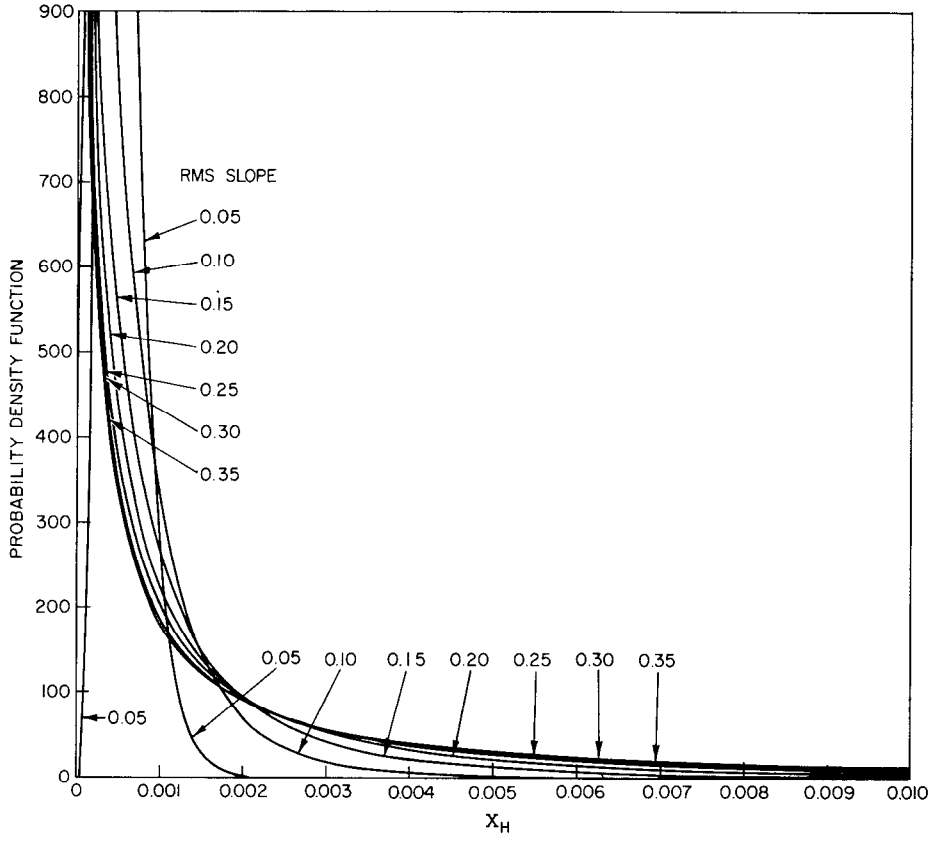

Fig. 3—Density function of X_H for perfectly conducting sea and 30-degree grazing angle

where $N = 8$ or 10 and the a_ℓ's are constants. Equations (22) and (36) can be used to obtain the general expression for the pdf of X:

$$p(X) \propto \frac{\sec^2 \tau}{8\sqrt{2\pi}\, S} \frac{\sum_{\ell=1}^{N} \ell a_\ell X^{(\ell-N)/N}}{\left(1 + \tan \tau \sum_{\ell=1}^{N} a_\ell X^{\ell/N}\right)^2} \cdot \exp\left(-\frac{1}{2S^2} \tan^2 \psi\right), \tag{37}$$

and the probability distribution corresponding to Eq. (37) is

$$P(X > X) \propto \frac{1}{2}\left\{ Erf\left(\frac{\cot \tau}{\sqrt{2}\, S}\right) \mp Erf\left(\frac{|\tan \psi|}{\sqrt{2}\, S}\right)\right\}, \tag{38}$$

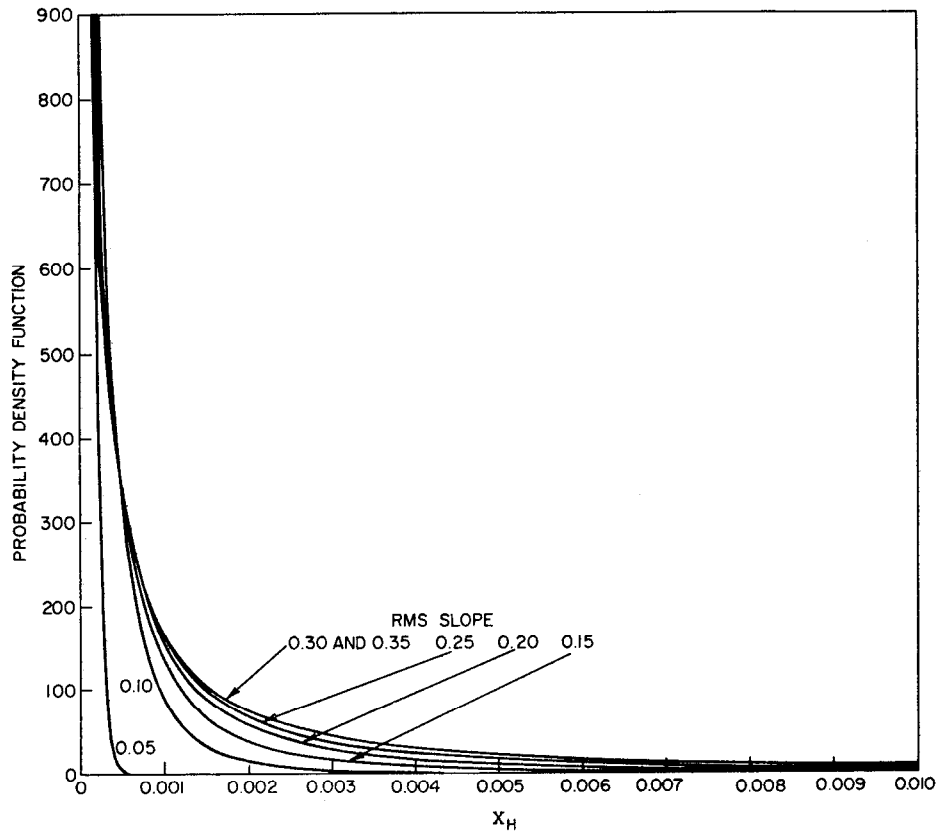

Fig. 4—Density function of X_H for perfectly conducting sea and 20-degree grazing angle

where again the upper sign applies for $\tan \psi \geq 0$ and the lower sign applies for $\tan \psi < 0$. In this case

$$\tan \psi = \frac{\sum_{\ell=1}^{N} a_\ell X^{\ell/N} - \tan \tau}{1 + \tan \tau \sum_{\ell=1}^{N} a_\ell X^{\ell/N}},$$

and the factor of proportionality in Eqs. (37) and (38), as before, is obtained from the normalization condition $P(X > 0) = 1$.

A more careful investigation of Eqs. (37) and (38) show that the distribution of X should tend toward the Gaussian distribution when the last few coefficients dominate (this is the case for vertical polarization). On the other hand if the first few coefficients dominate in Eq. (36), the distribution of X should tend toward the lognormal distribution (this is the case for horizontal polarization. Thus, this model predicts that sea clutter for horizontal polarization should tend toward the lognormal distribution.

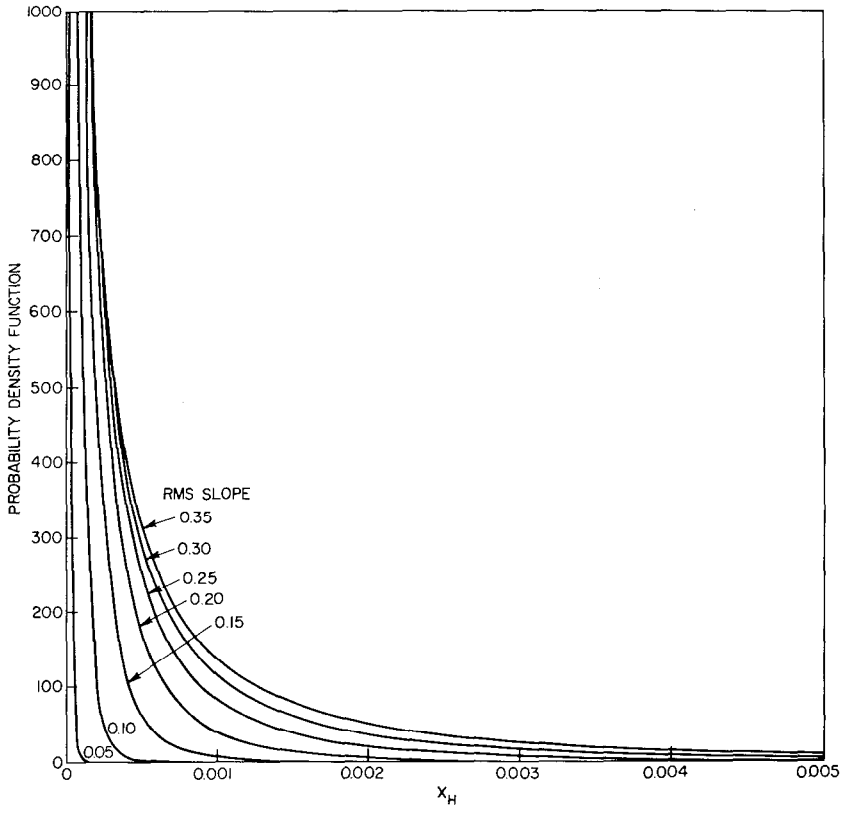

Fig. 5—Density function of X_H for perfectly conducting sea and 10-degree grazing angle

Of course, the statistics of sea clutter in final analysis is related to the distribution of the random variable Z which also depends on the distribution of the other random variable Y, which in our model is always an exponential distribution. Thus, any lognormal characteristics of sea-clutter distribution must come from the distribution of the random variable X. In general closed-form expressions cannot be obtained for the pdf and distribution function of Z.

However, some limiting properties can be derived for the distribution of Z. For example, take the case of a glassy sea (no undulating function is present, $S = 0$). Clearly the pdf of X will be a delta function:

$$p(X) = \delta(X - \overline{X}) \tag{39}$$

and

$$p(Z) = \frac{1}{\overline{X}} e^{-Z/X}, \tag{40}$$

where $\overline{X}$ is the mean value of X and also of Z, and Z is exponentially distributed for this case.

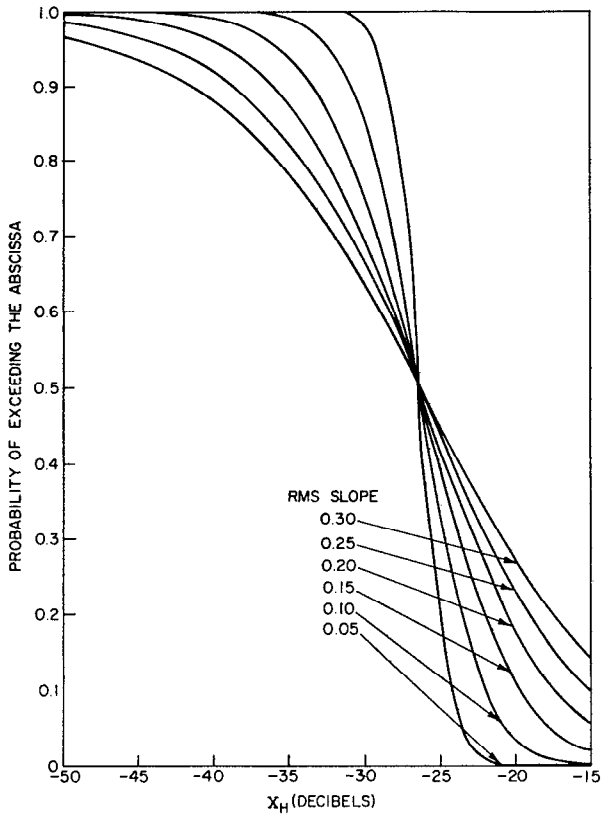

Fig. 6—Distribution function of X_H for perfectly conducting sea and 40-degree grazing angle

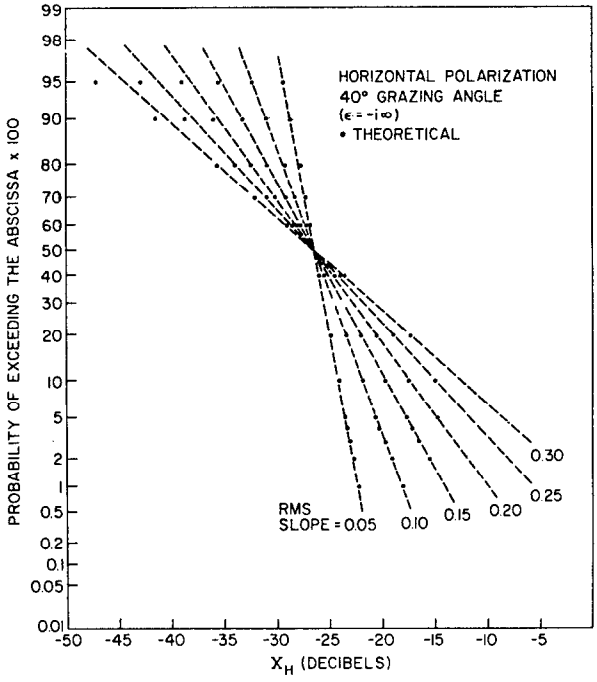

Fig. 7—Distribution function of X_H for perfectly conducting sea and 40-degree grazing angle, in normal probability paper

For increasing value of S (rougher seas), $p(X)$ should develop a longer tail (see Figs. 2-5); thus, $p(Z)$ will also have a longer tail, which should make the distribution of Z tend toward the lognormal distribution (in particular for horizontal polarization).

The moments of Eqs. (33), (34), and (37) do not exist because we have used a K^{-4} spectrum which has a singularity at $K = 0$. This in principle can be corrected by cutting off the spectrum before $K = 0$. A shadowing function may also be included in Eq. (21) but has not been attempted here.

IDENTIFICATION OF THE STATISTICS OF SEA CLUTTER OBTAINED WITH THE NRL-4FR SYSTEM

Quantitative analysis of sea clutter statistics is necessary for further development and improvement of the statistical model of sea clutter. Thus, analysis has been performed on sea-clutter data taken with the 4FR system which generally uses pulse widths between 0.1 and 0.5 μsecond and whose antenna beamwidths are greater than 5 degrees. Accordingly the illuminated area in this case contains many "patches" and no direct comparisons will be possible with the predictions of the statistical model, but any statistical information obtained for sea clutter will be helpful in assessing or updating the statistical model.

A detailed description of the 4FR system has already been given by Guinard (8); thus, here we should only indicate that the samples of sea clutter used in this investigation are samples of backscattered power (or radar cross section of the sea) which have been collected by a logarithmic receiver with a dynamic range of over 45 decibels. The output of the receiver is digitalized by means of a 30-nanosecond gate to seven-bit accuracy. The sea conditions and radar parameters of the measurements are summarized in Table 1. The experiment in the North Atlantic during February 1969 was performed in the neighborhood of Ocean Stations India and Juliet.

The Distribution Function

The samples of sea clutter, for depression angles of 5 to 30 degrees, taken with the 4FR system have been distributed and checked with the Kolmogorov-Smirnov test (17) if they come from an exponential population (Rayleigh envelope) or a lognormal population. In fitting the exponential distribution, the mean value of the exponential distribution was adjusted for a minimum-maximum deviation between the sample and the population distribution. In fitting the lognormal distribution, the variance and the median values were taken to be those of the sample.

The number of independent samples of sea clutter was estimated by means of a standard run-test (18) in an application of the Wald-Wolfowitz test (19). The procedure used here is identical to that described by Schmidt (20) except that in our investigation sets of 1024 samples are used instead of 2048. The run-test, using the 95% level of significance, shows that 1 out of 4 samples is independent for X band, 1 out of 8 or 9 for C band, 1 out of 35 for L band, and 1 out of 120 to 130 is independent for P band. Of course, these are average numbers; in the analysis the exact number of independent samples was used for each

Table I
Radar and Sea Conditions

Date	Wind Speed (m/sec)	Wave Height (m)	Location	Altitude (m)	Indicated Air Speed (m/sec)	Pulse Rep. Rate (pps)	Pulse Width (μsec)
2/11/69	24.5	8.0	OWS "I"	480	97	683	0.5
2/13/69	18	7.0	OWS "J"	460	103	603	0.5
2/14/69	20	7.5	OWS "J"	460	103	603	0.5
2/17/69	2.5	4.6	OWS "I"	410	103	603	0.5
2/18/69	11	3.0	OWS "J"	460	103	603	0.5
1/23/70	6.2	3.7	Bermuda	180	103-115	683	0.5
1/26/70	7.5	1.5	Bermuda	750	89-108	683	0.5
1/27/70	8.2	1.8	Bermuda	180	87-108	683	0.5
1/27/70	8.2	1.8	Bermuda	610	87-110	683	0.5

cumulative distribution and in general the number of independent samples is proportional to the radar frequency. No specific trends were found with polarization; the motion of the aircraft is expected to decorrelate the samples of sea clutter faster. Thus, for sea clutter taken with a stationary radar the number of independent samples should be smaller.

The Kolmogorov-Smirnov test, either at the 99% or at the 80% level of significance, shows that for calm seas and small sample sizes the cumulative distributions of sea clutter are acceptable as exponential or lognormal. However, for large sample sizes (data up to 30 seconds in this case) the maximum deviation between the distributions becomes larger than the acceptable limit and should be rejected as belonging to the exponential or the lognormal family, with the smaller maximum deviations obtained against the exponential distribution in most cases.

The maximum deviations for *P*- and *L*-band data were in general smaller than the maximum deviations for *C*- and *X*-band data when compared with the exponential and the lognormal distributions. A trend occurs with polarization which may be more obvious in terms of the central moments, which are investigated in the next section.

In Figs. 8a-8x, some typical maximum deviations illustrate the above conclusions. In these figures, only the comparison with the exponential distribution is shown. The maximum deviations in comparison with the lognormal distribution are not too different than those shown, except that, in general, they tend to be a little greater.

The outcome of the Kolmogorov-Smirnov test, although conclusive, is not very satisfying since the statistics of sea clutter are still not known.

The Central Moments

The Kolmogorov-Smirnov test has demonstrated that sea clutter taken with the 4FR system is not exponential nor lognormal distributed. To obtain a quantitative estimate of these statistics, the first five central moments of sea clutter should be computed from the data, in decibels, to avoid additional errors in scaling of the data.

The central moments $\mu_1, \mu_2, ..., \mu_n$ of a random variable which is exponentially or lognormal distributed are well known and can be used for comparison. The central moments for the logarithm of a random variable which is exponentially distributed are related to the poligamma function (21)

$$\psi^{(\nu-1)} = \frac{d^\nu}{dX^\nu} [\ln \Gamma(x+1)], \tag{41}$$

(where $\Gamma(x+1)$ is the gamma function). The central moments are:

$$\left.\begin{aligned} \mu_2 &= \psi^{I} \quad (0) = \quad 1.64493 \\ \mu_3 &= \psi^{II} \quad (0) = -\ 2.40411 \\ \mu_4 &= \psi^{III} \quad (0) = \quad 6.49393 \\ \mu_5 &= \psi^{IV} \quad (0) = -24.88627 \end{aligned}\right\} \tag{42}$$

and $\psi(0) = -0.5772157$ is related to the difference between the natural logarithm of the mean value of the exponential distribution and the mean value of the natural logarithm of the random variable. The numerical values of the poligamma function have been obtained from Davis (22).

The central moments of the logarithm of a random variable which has a lognormal distribution are those of the Gaussian distribution (14)

$$\mu_n = 1 \cdot 3 \cdot 5 ... (n-1) \mu_2{}^{n/2}, \tag{43}$$

where $n \geq 2$ and is even. If n is odd, $\mu_n = 0$.

In Figs. 9 and 10 the pdf and the distribution function of an exponential and a lognormal random variable have been sketched for comparison.

Figures 11 through 20 illustrate the (median, mean) difference and the first five central moments of sea clutter (in decibels) taken with the NRL-4FR system for moderate and rough sea conditions. These figures also show the corresponding values for the exponential and lognormal distribution. As observed the central moments of sea clutter are in most cases intermediate between those of the exponential (Rayleigh envelope) and those of the lognormal distribution, except for the fourth central moment.

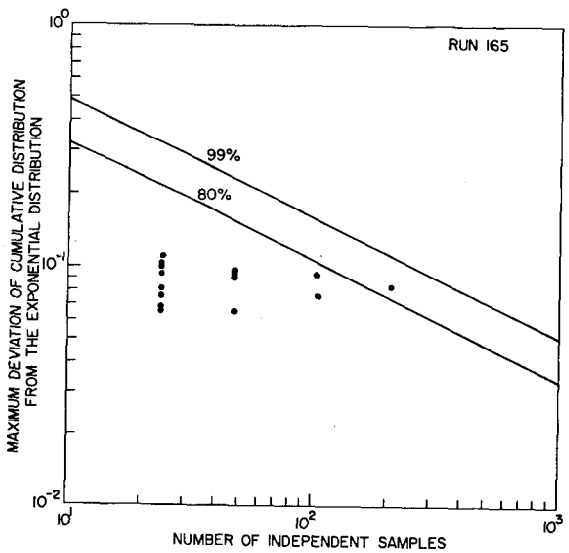

(a) Vertical polarization of P band on Feb. 11, 1969

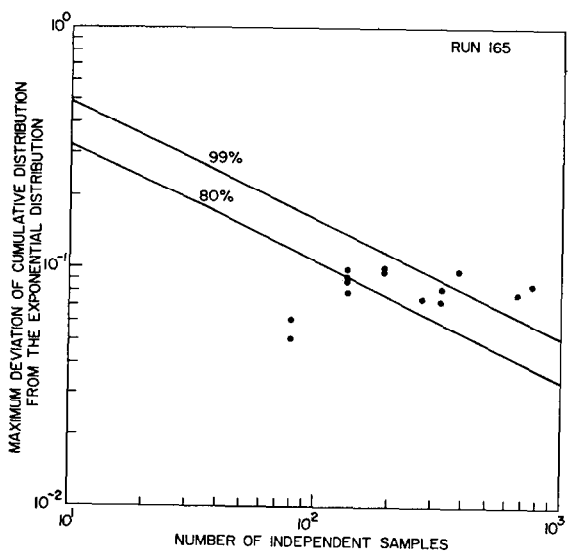

(b) Vertical polarization of L band on Feb. 11, 1969

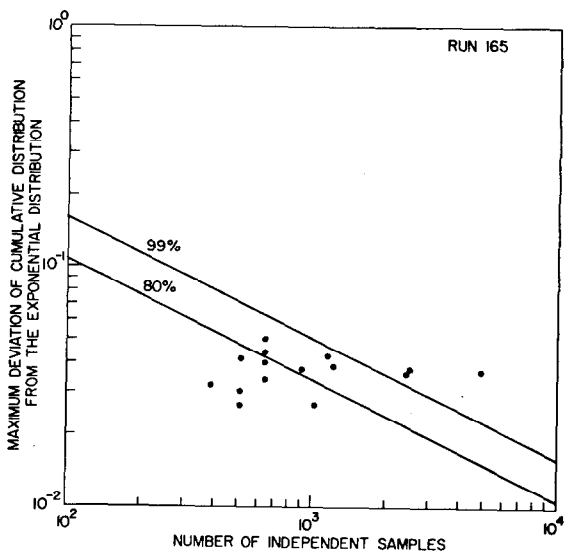

(c) Vertical polarization of C band on Feb. 11, 1969

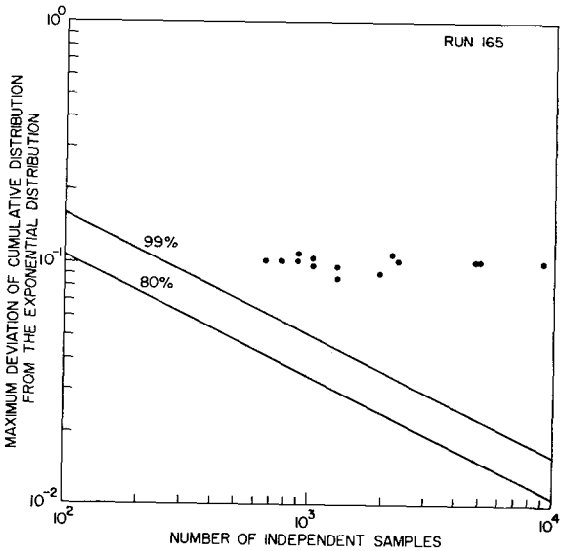

(d) Vertical polarization of X band on Feb. 11, 1969

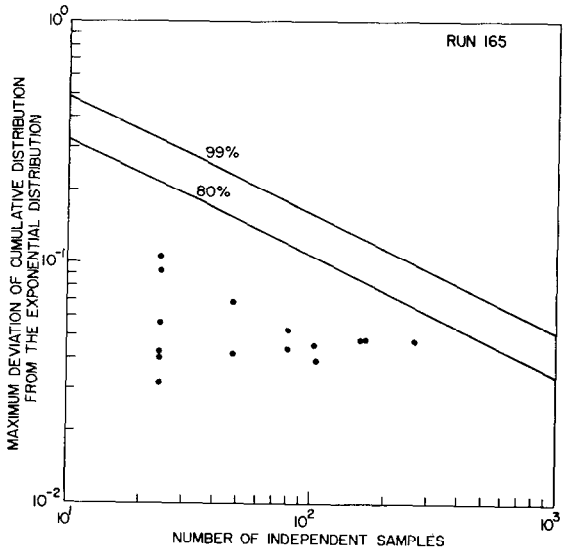

(e) Horizontal polarization of P band on Feb. 11, 1969

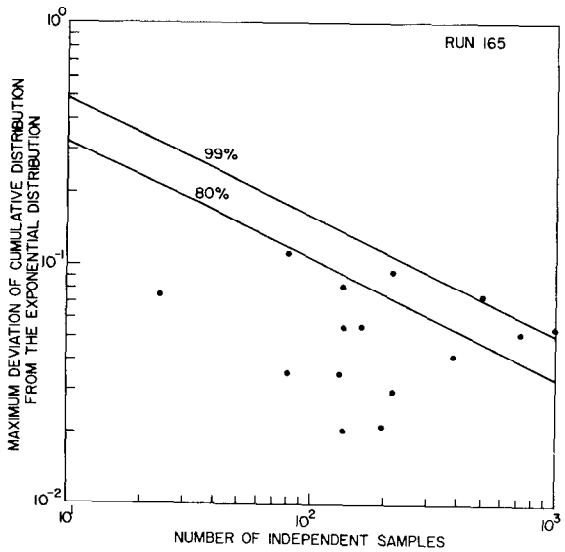

(f) Horizontal polarization of L band on Feb. 11, 1969

Fig. 8—Maximum deviation of cumulative distribution of sea clutter, taken with the 4FR system, from the exponential distribution (Rayleigh envelope), with the 99% and 80% levels of significance from the Kolmogorov-Smirnov test

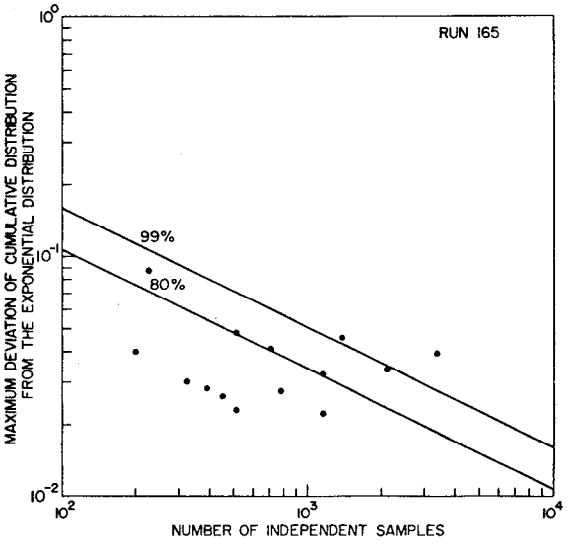

(g) Horizontal polarization of C band on Feb. 11, 1969

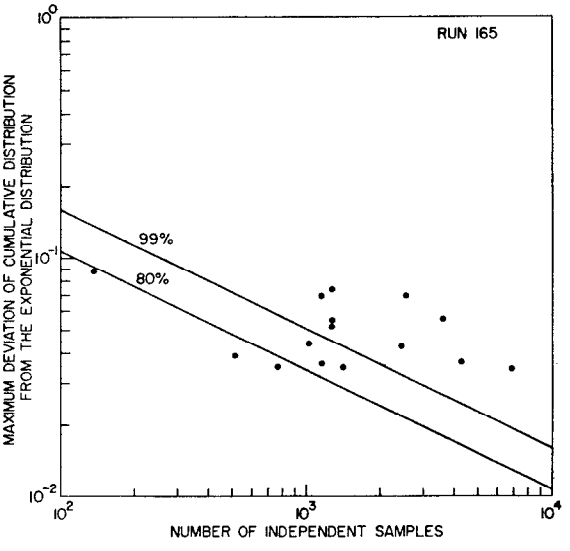

(h) Horizontal polarization of X band on Feb. 11, 1969

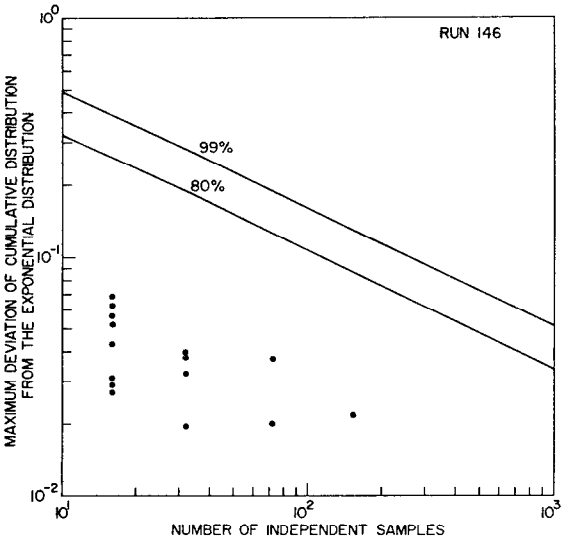

(i) Vertical polarization of P band on Jan. 26, 1970

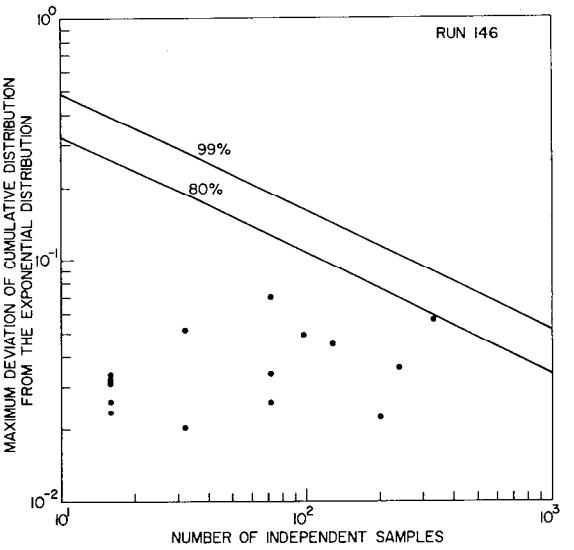

(j) Vertical polarization of L band on Jan. 26, 1970

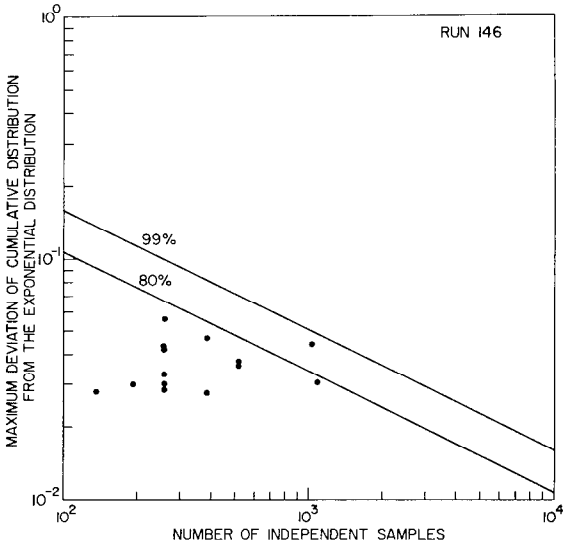

(k) Vertical polarization of C band on Jan. 26, 1970

(l) Vertical polarization of X band on Jan. 26, 1970

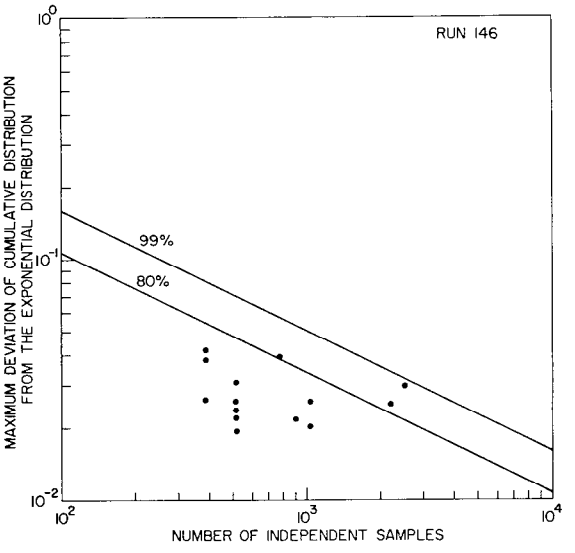

Fig. 8—Maximum deviation of cumulative distribution of sea clutter, taken with the 4FR system, from the exponential distribution (Rayleigh envelope), with the 99% and 80% levels of significance from the Kolmogorov-Smirnov test

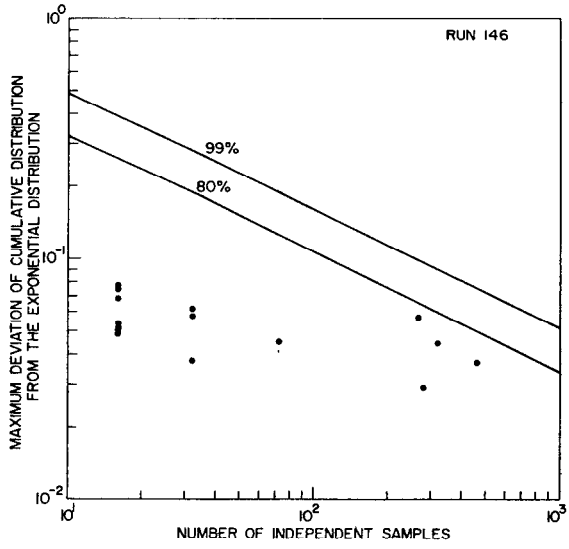

(m) Horizontal polarization of P band on Jan. 26, 1970

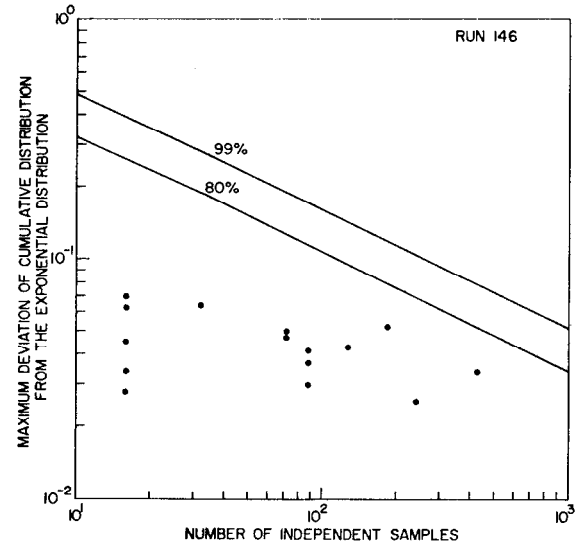

(n) Horizontal polarization of L band on Jan. 26, 1970

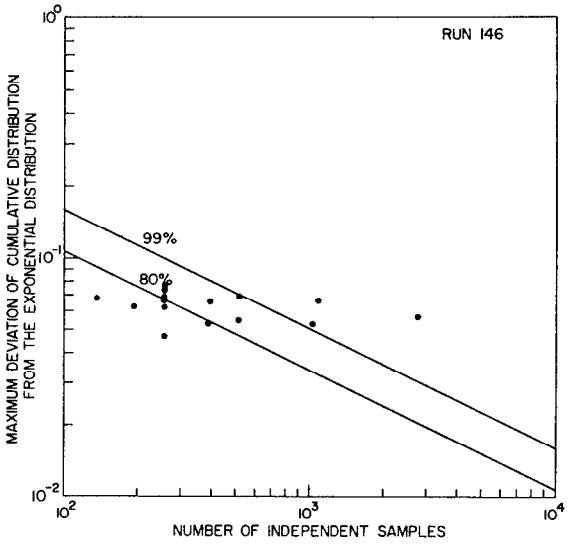

(o) Horizontal polarization of C band on Jan. 26, 1970

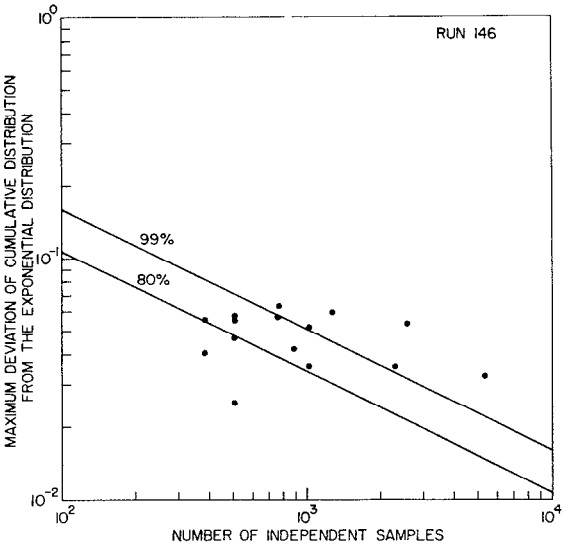

(p) Horizontal polarization of X band on Jan. 26, 1970

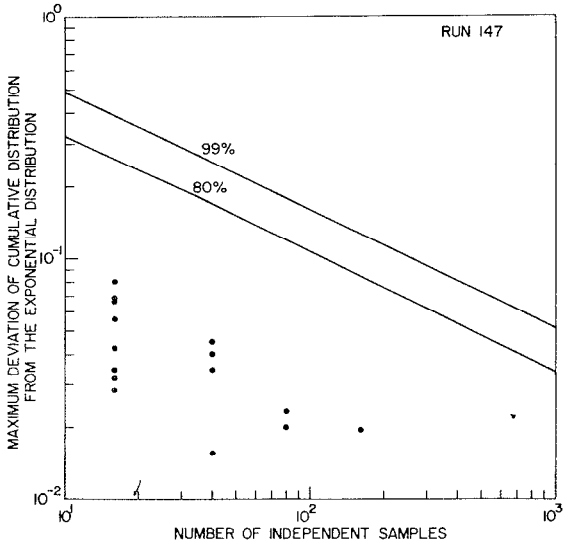

(q) Vertical polarization of P band on Jan. 26, 1970

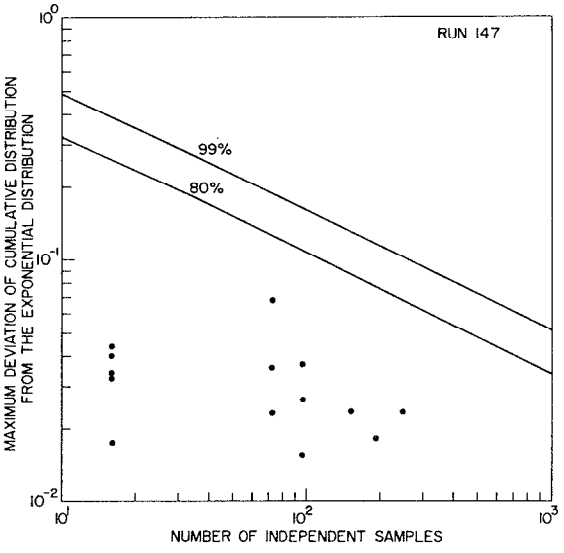

(r) Vertical polarization of L band on Jan. 26, 1970

Fig. 8—Maximum deviation of cumulative distribution of sea clutter, taken with the 4FR system, from the exponential distribution (Rayleigh envelope), with the 99% and 80% levels of significance from the Kolmogorov-Smirnov test

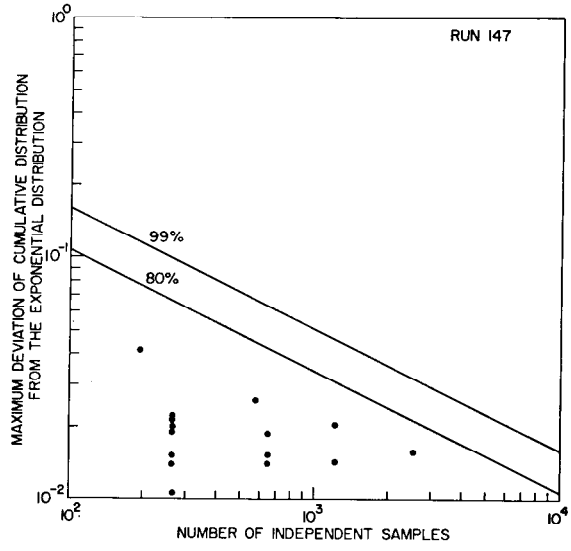

(s) Vertical polarization of C band on Jan. 26, 1970

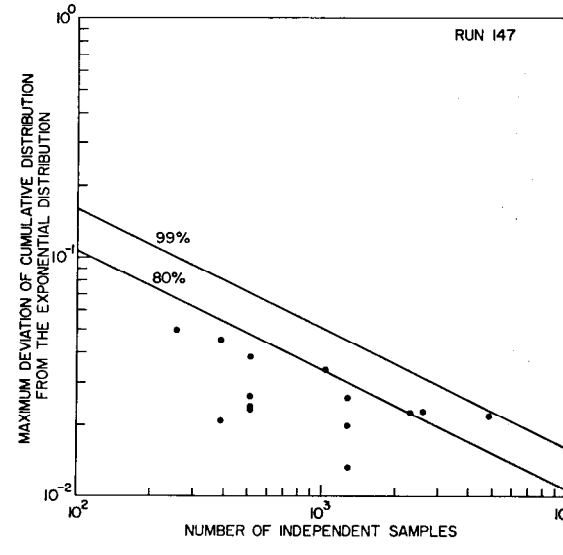

(t) Vertical polarization of X band on Jan. 26, 1970

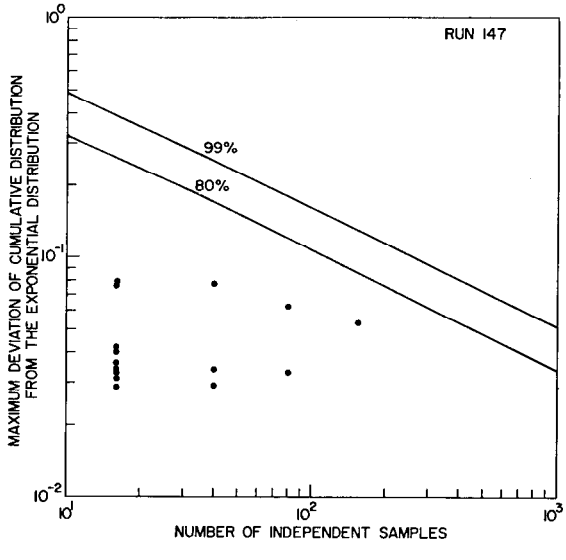

(u) Horizontal polarization of P band on Jan. 26, 1970

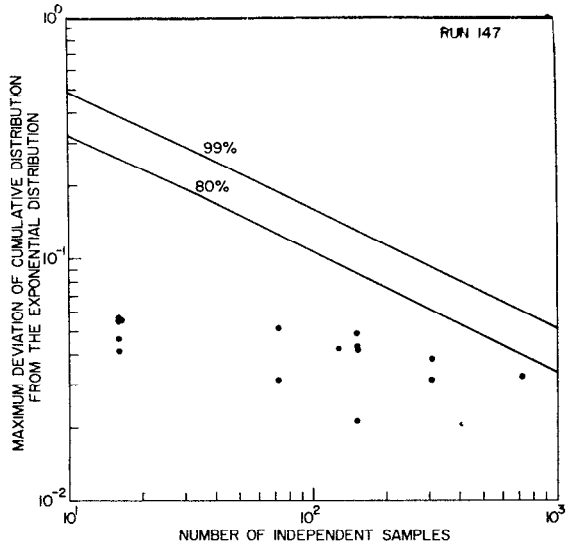

(v) Horizontal polarization of L band on Jan. 26, 1970

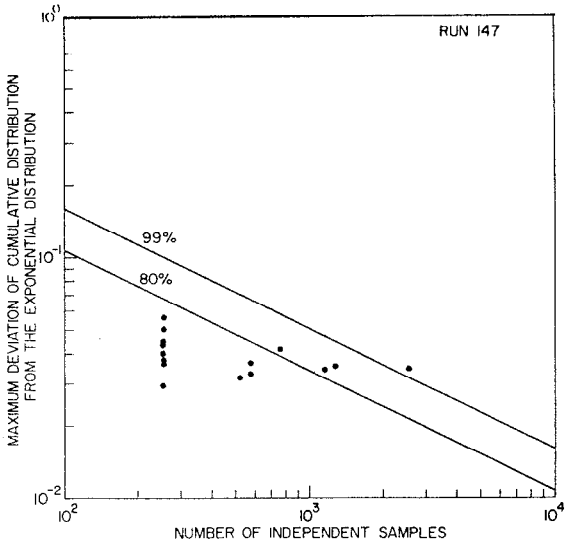

(w) Horizontal polarization of C band on Jan. 26, 1970

(x) Horizontal polarization of X band on Jan. 26, 1970

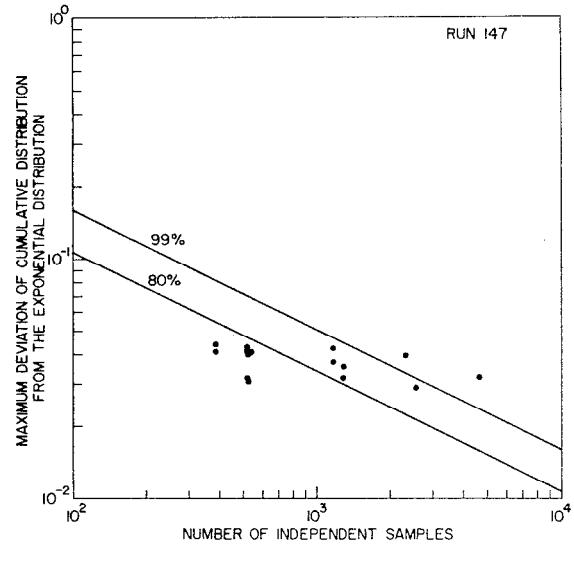

Fig. 8—Maximum deviation of cumulative distribution of sea clutter, taken with the 4FR system, from the exponential distribution (Rayleigh envelope), with the 99% and 80% levels of significance from the Kolmogorov-Smirnov test

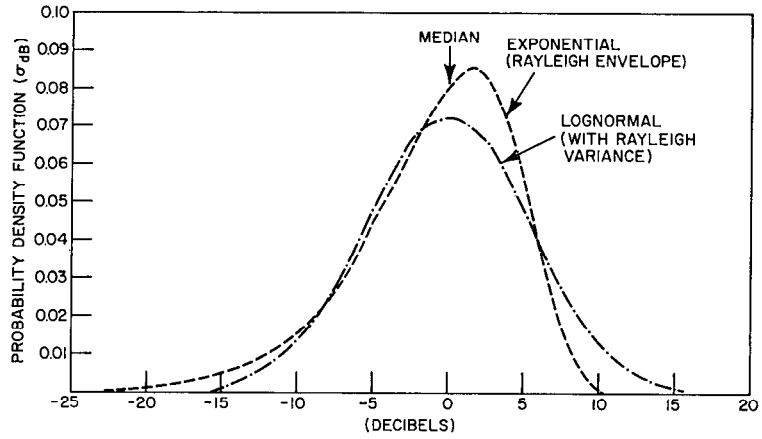

Fig. 9—Comparison of the exponential (Rayleigh envelope) and the lognormal density functions

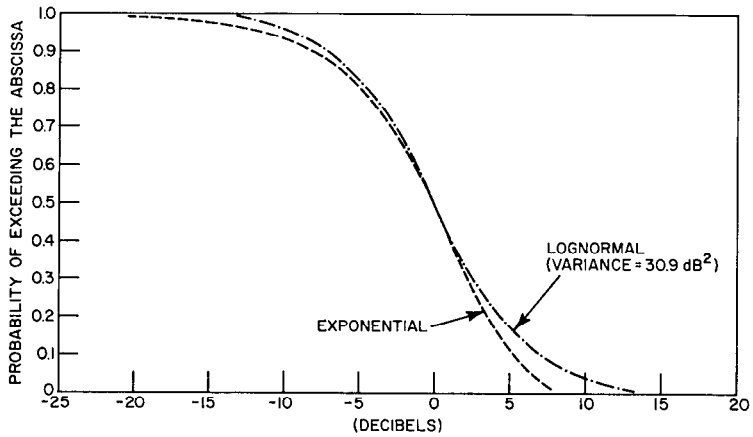

Fig. 10—Comparison of the exponential (Rayleigh envelope) and the lognormal distribution functions

The central moments for vertical polarization are nearer to those for the exponential distribution, which agrees with the prediction of the model for the statistics of sea clutter. It would seem that the wide spread in the magnitude of the central moments may be an indication that in general sea clutter is not stationary. Temporal variation of sea clutter has been investigated by Schmidt (20).

With the central moments obtained for sea clutter, the true pdf and distribution functions should be reconstructable with no difficulty.

DISCUSSION OF RESULTS AND CONCLUSIONS

A model for the statistics of sea clutter has been developed using scattering theory and the composite surface-scattering model, which uses the assumption that the rough

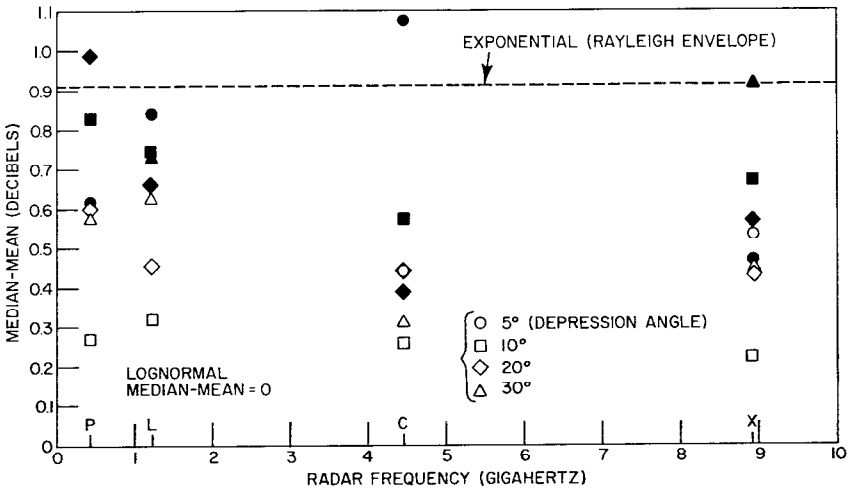

Fig. 11—Median, mean difference of sea clutter taken with the 4FR system for moderate seas. The wind speed was 5 to 10 meters/second. Solid points represent vertical polarization and open points, horizontal polarization.

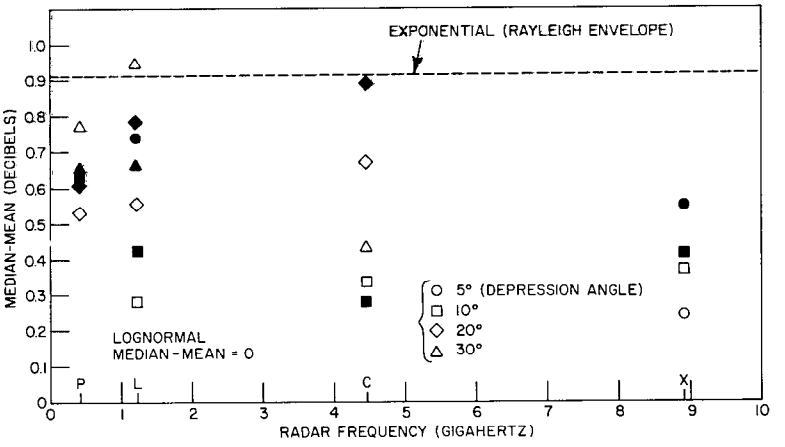

Fig. 12—Median, mean difference of sea clutter taken with the 4FR system for rough seas. The wind speed was 15 to 20 meters/second. Solid points represent vertical polarization and open points, horizontal polarization

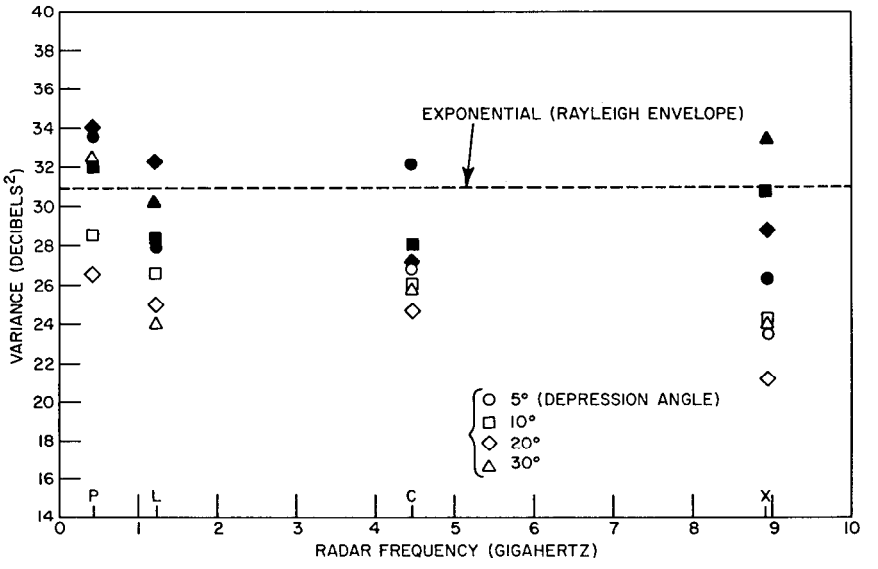

Fig. 13—Variance of sea clutter taken with the 4FR system for moderate seas. The wind speed was 5 to 10 meters/second. The solid points represent vertical polarization and the open points, horizontal polarization.

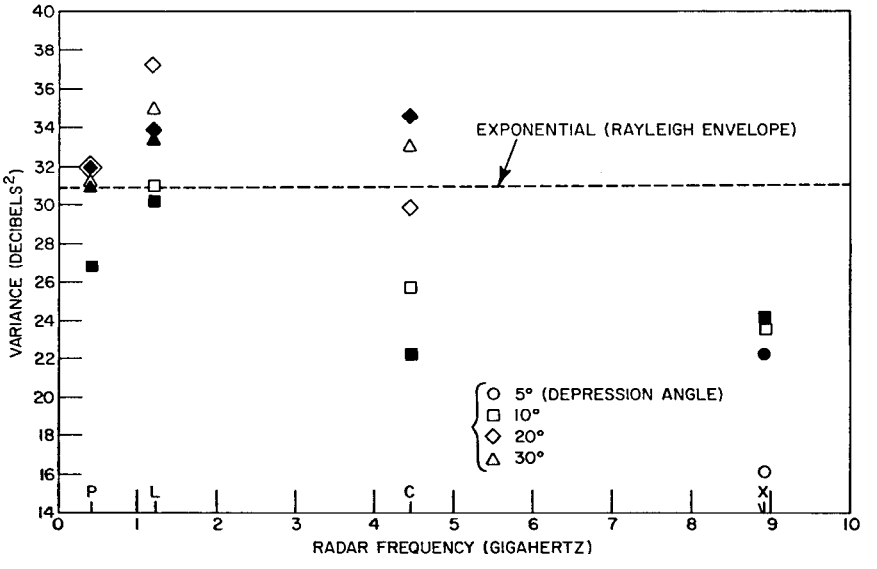

Fig. 14—Variance of sea clutter taken with the 4FR system for rough seas. The wind speed was 15 to 20 meters/second. The solid points represent vertical polarization and open points, horizontal polarization.

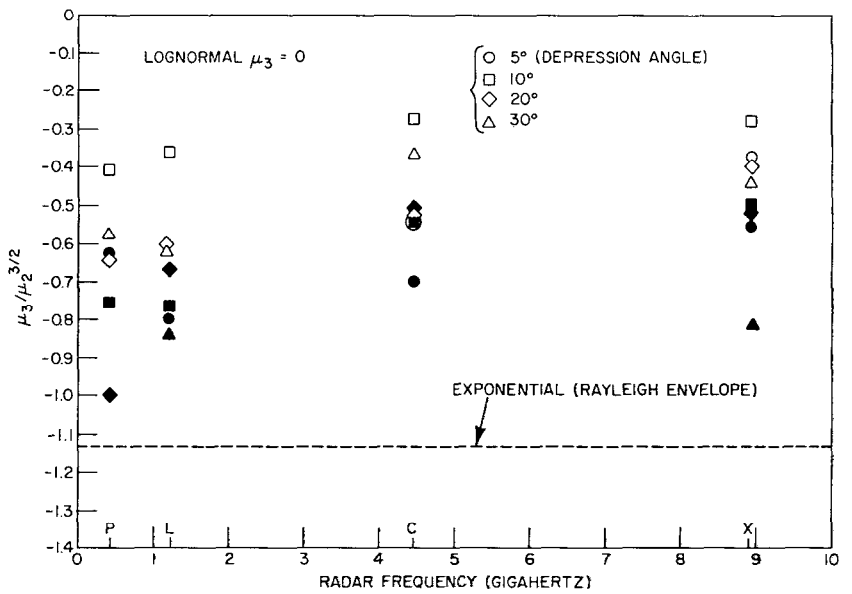

Fig. 15—Third central moment of sea clutter taken with the 4FR system for moderate seas. The wind speed was 5 to 10 meters/second. The solid points represent vertical polarization and the open points, horizontal polarization.

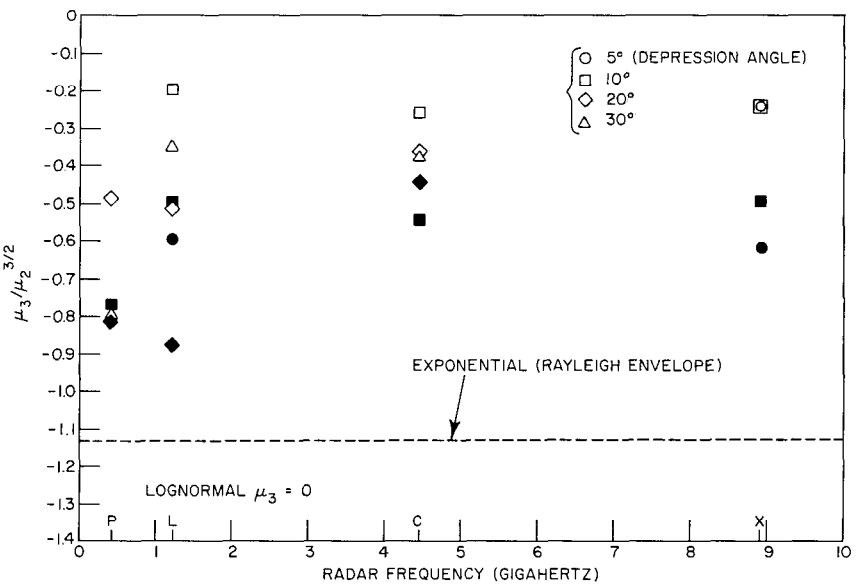

Fig. 16—Third central moment of sea clutter taken with the 4FR system for rough seas. The wind speed was 15 to 20 meters/second. The solid points represent vertical polarization and the open points, horizontal polarization.

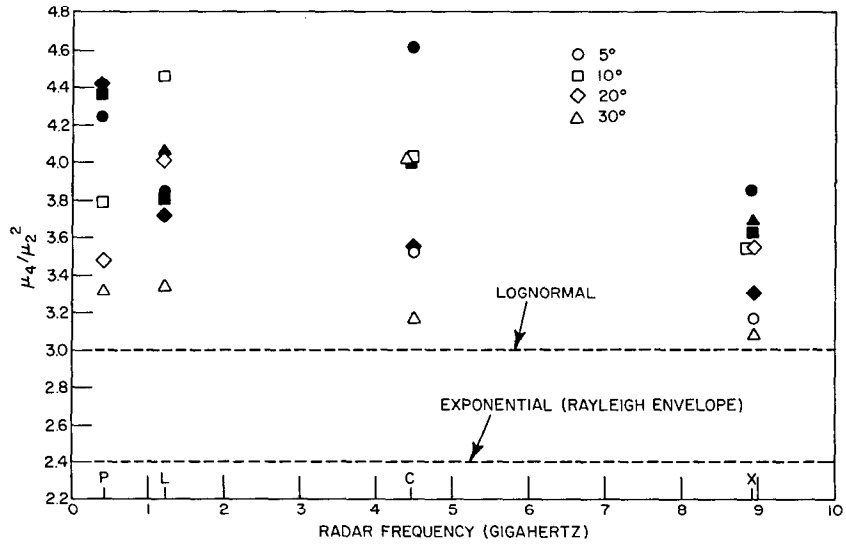

Fig. 17—Fourth central moment of sea clutter taken with the 4FR system for moderate seas. The wind speed was 5 to 10 meters/second. The solid points represent vertical polarization and the open points, horizontal polarization.

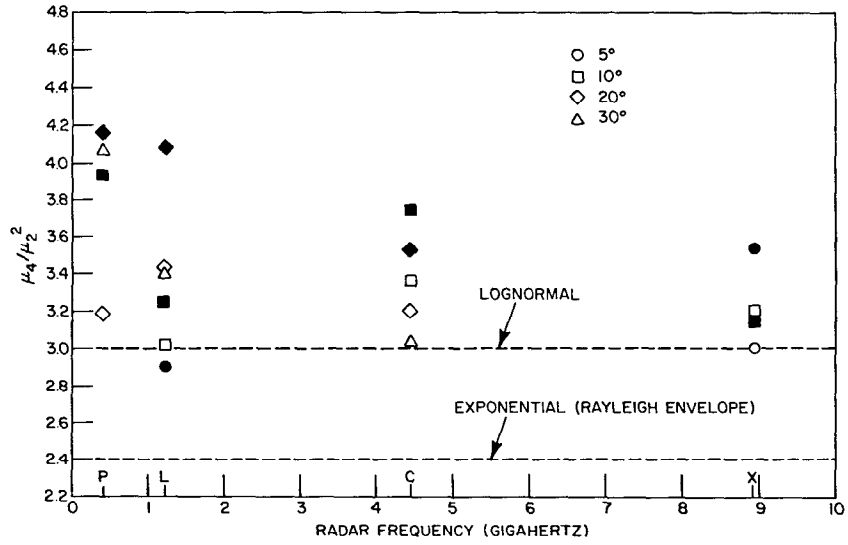

Fig. 18—Fourth central moment of sea clutter taken with the 4FR system for rough seas. The wind speed was 15 to 20 meters/second. The solid points represent vertical polarization and the open points, horizontal polarization.

surface "locally" is slightly rough. For the sea the "local"-slightly rough assumption is quite a reasonable approximation at most conventional radar frequencies.

The case of single "patch" illumination is treated in detail, with the model predicting the statistics of sea clutter to be exponential (Rayleigh envelope) for a glassy sea (no large-scale roughness present), and for increasing roughness the distribution should develop a longer tail similar to that for a lognormal distribution, in particular for horizontal polarization. Obviously, a mechanism has been found that yields sea clutter with a distribution of lognormal character.

Beckmann (23) has shown that by using physical optics for a perfectly conducting rough surface the scattered fields should be Rayleigh distributed everywhere except near the specular direction, and for very rough surfaces the scattered fields should be Rayleigh distributed even in the specular direction. Thus, the non-Rayleigh statistics are obviously due to the scattering properties of the slightly rough "patches" and the tilting of the "patches" by the large-scale roughness.

As future input for updating the model, the statistics of sea clutter taken with the 4FR system have been analyzed by the Kolmogorov-Smirnov test and by a computation of the central moments of the distribution. The results indicate that in general sea clutter is not exponentially (Rayleigh envelope) nor lognormally distributed, and these distributions may only be the limiting distributions of sea clutter. The large spread of the central moments may be an indication that sea clutter is not stationary; therefore, the optimum radar detector must be of an adaptive nature.

Some other important results obtained in the empirical identification of sea clutter are:

1. For large sample sizes (greater than about 1000 independent samples) sea clutter is not exponential nor lognormal,

2. For small sample sizes (less than 200 independent samples) sea-clutter statistics may be approximated by both the exponential and the lognormal distributions,

3. Sea clutter for vertical polarization, in general, is more exponential than sea clutter for horizontal polarization,

4. Sea clutter for P and L band, in general, is more exponential than sea clutter for C and X band,

5. The number of independent samples is roughly proportional to radar frequency,

6. Sea clutter for calm seas is more exponential than sea clutter for rougher seas.

In conclusion, it is possible to say that the model developed for the statistics of sea clutter and the empirical identification of data taken with the 4FR system indicate that the distribution of sea clutter is intermediate between the exponential (Rayleigh envelope) and the lognormal distribution. Accordingly, the expected probability of false alarm for radars

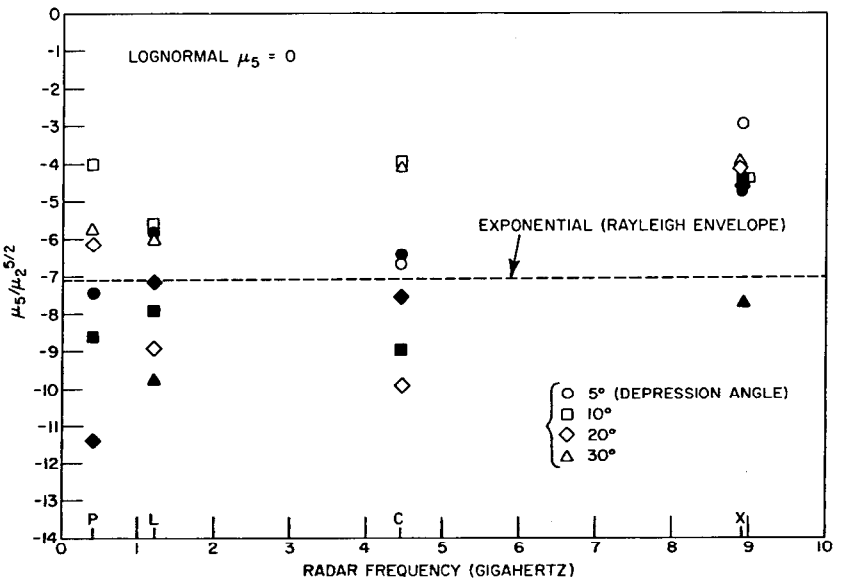

Fig. 19—Fifth central moment of sea clutter taken with the 4FR system for moderate seas. The wind speed was 5 to 10 meters/second. The solid points represent vertical polarization and the open points, horizontal polarization.

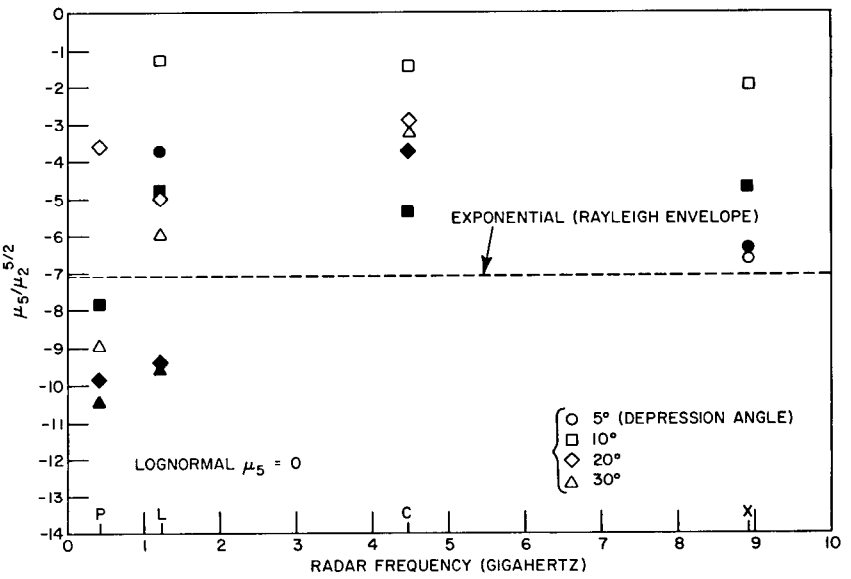

Fig. 20—Fifth central moment of sea clutter, taken with the 4FR system, for rough seas. The wind speed was 15 to 20 meters/second. The solid points represent vertical polarization and the open points, horizontal polarization.

operating in the sea environment should be larger than that predicted for an exponentially distributed clutter, in particular for horizontal polarization and toward grazing incidence.

ACKNOWLEDGMENTS

The authors thank N. W. Guinard for suggesting the application of the composite surface-scattering model to investigating the statistics of sea clutter.

REFERENCES

1. D. Middleton, *An Introduction to Statistical Communication Theory*, McGraw-Hill, New York, 1960.

2. J.I. Marcum, "A Statistical Theory of Target Detection by Pulsed Radar," Rand Corp., Santa Monica, Calif., RM-754, Dec. 1, 1947, and RM-753, July 1, 1948.

3. P. Swerling, "Probability of Detection for Fluctuating Targets," Rand Corp., Santa Monica, Calif., RM-1217, Mar. 17, 1954, and IRE Trans. Inform. Theory, *IT-6*, 269-308 (1960).

4. H.L. Van Trees, *Detection, Estimation, and Modulation Theory*, Wiley, New York, 1968.

5. G.V. Trunk and S.F. George, "Detection of Targets in Non-Gaussian Sea Clutter," IEEE Trans., *AES-6*, No. 5, 620-628 (1970).

6. J.W. Wright, "A New Model for Sea Clutter," IEEE Trans. *AP-16*, No. 2, 217-223 (1968).

7. G.R. Valenzuela, "Scattering of Electromagnetic Waves from a Tilted Slightly Rough Surface," Radio Sci. *3*, No. 11, 1057-1066 (1968).

8. N.W. Guinard, "The NRL Four-Frequency Radar System," Report of NRL Progress, May 1969, pp. 1-10.

9. N.W. Guinard and J.C. Daley, "An Experimental Study of a Sea Clutter Model," Proc. IEEE *58*, No. 4, 543-550 (1970).

10. N.W. Guinard, J.T. Ransone, Jr., and J.C. Daley, "The Variation of the NRCS of the Sea with Increasing Roughness," J. Geophys. Res. *76*, No. 6, 1525-1538 (1971).

11. G.R. Valenzuela, M.B. Laing, and J.C. Daley, "Ocean Spectra for the High Frequency Waves as Determined from Airborne Radar Measurements," J. Marine Res. *29*, No. 2, 69-84 (1971).

12. G.R. Valenzuela and M.B. Laing, "Study of Doppler Spectra of Radar Sea Echo," J. Geophys. Res. *75*, No. 3, 551-563 (1970).

13. A.W. Maue, "Zur Formulierung eines allgemeinen Beugungsproblems durch eine Integralgleichung," Z. Physik *126*, 601-618 (1949).

14. K.M. Mitzner, "An Integral Equation Approach to Scattering from a Body of Finite Conductivity," Radio Sci. *2*, No. 12, 1459-1470 (1967).

15. F.G. Bass, I.M. Fuks, A.I. Kalmykov, I.E. Ostrovsky, and A.D. Rosenberg, "Very High Frequency Radiowave Scattering by a Distrubed Sea Surface," Trans. IEEE *AP-16*, No. 5, 554-568 (1968).

16. W.B. Davenport, Jr., and W.L. Root, Chapter 3 in *An Introduction to the Theory of Random Signals and Noise*, McGraw-Hill, New York, 1958.

17. F.J. Massey, Jr., "The Kolmogorov-Smirnov Test for Goodness of Fit," J. Am. Stat. Assoc. *46*, 68-78 (1951).

18. J.S. Bendat and A.G. Piersol, *Measurement and Analysis of Random Data*, Wiley, New York, 1966.

19. A. Wald and J. Wolfowitz, "On a Test Whether Two Samples are from the Same Population," Ann. Math. Stat. *11*, 147-162 (1940).

20. K.R. Schmidt, "Statistical Time-Varying and Distribution Properties of High-Resolution Radar Sea Echo," NRL Report 7150, Nov. 9, 1970.

21. M.M. Siddigui, "Statistical Inference for Rayleigh Distributions," Radio Science (Journal of Research NBS/USNC-URSI) *68D*, No. 9, 1005-1010 (1968).

22. H.T. Davis, *Tables of the Mathematical Functions*, Vol. II, The Principia Press of Trinity University, San Antonio, Texas, 1935.

23. P. Beckmann and A. Spizzichino, Chapter 7 *The Scattering of Electromagnetic Waves from Rough Surfaces*, New York, Pergamon Press, 1963.